Cerebral Cortex January 2005;15:31-39
doi:10.1093/cercor/bhh105
Advance Access publication July 6, 2004

Functional–Anatomical Validation and Individual Variation of Diffusion Tractography-based Segmentation of the Human Thalamus

Heidi Johansen-Berg[1], Timothy E.J. Behrens[1], Emma Sillery[1], Olga Ciccarelli[2], Alan J. Thompson[2], Stephen M. Smith[1] and Paul M. Matthews[1]

[1]Centre for Functional Magnetic Resonance Imaging of the Brain, University of Oxford, John Radcliffe Hospital, Oxford OX3 9DU, UK and [2]Institute of Neurology, Queen Square, University College London, London WC1N 3BG, UK

Parcellation of the human thalamus based on cortical connectivity information inferred from non-invasive diffusion-weighted images identifies sub-regions that we have proposed correspond to nuclei. Here we test the functional and anatomical validity of this proposal by comparing data from diffusion tractography, cytoarchitecture and functional imaging. We acquired diffusion imaging data in eleven healthy subjects and performed probabilistic tractography from voxels within the thalamus. Cortical connectivity information was used to divide the thalamus into sub-regions with highest probability of connectivity to distinct cortical areas. The relative volumes of these connectivity-defined sub-regions correlate well with volumetric predictions based on a histological atlas. Previously reported centres of functional activation within the thalamus during motor or executive tasks co-localize within atlas regions showing high probabilities of connection to motor or prefrontal cortices, respectively. This work provides a powerful validation of quantitative grey matter segmentation using diffusion tractography in humans. Co-registering thalamic sub-regions from 11 healthy individuals characterizes inter-individual variation in segmentation and results in a population-based atlas of the human thalamus that can be used to assign likely anatomical labels to thalamic locations in standard brain space. This provides a tool for specific localization of functional activations or lesions to putative thalamic nuclei.

Keywords: atlas, cytoarchitecture, diffusion imaging, FMRI, neocortex

Introduction

The ability to parcellate the human thalamus into meaningful subdivisions *in vivo* would have significant implications for the study of normal brain function and for investigation of disorders associated with thalamic pathology. Activation of the thalamus has been observed in a number of functional imaging studies involving various sensory (Davis *et al.*, 1998), motor (Samuel *et al.*, 1997; Krams *et al.*, 1998) and cognitive (Baker *et al.*, 1996; LaBar *et al.*, 1999; Dove *et al.*, 2000) tasks, but lack of detailed anatomical information in the thalamus has limited structure–function correlations. Lesions of the thalamus can have wide-ranging effects on sensory, executive and memory functions (Wallesch *et al.*, 1983; von Cramon *et al.*, 1985; Van der Werf *et al.*, 2003) and involvement of thalamo-cortical circuitry is thought to be crucial in certain neurological and psychiatric disorders (Modell *et al.*, 1989; Andreasen *et al.*, 1996). Borders between cytoarchitectonically defined thalamic nuclei can only be definitively determined post-mortem.

However, each thalamic nucleus has a distinct pattern of cortical and subcortical connectivity (Van Buren and Burke, 1972; Jones, 1985; Goldman-Rakic and Porrino, 1985; Yeterian and Pandya, 1985, 1988, 1991, 1997; Darian-Smith *et al.*, 1990; Guillery and Sherman, 2002). We have previously exploited this fact to parcellate the human thalamus *in vivo* on the basis of its cortical connectivity (Behrens *et al.*, 2003a). Our approach uses diffusion-weighted magnetic resonance images to perform probabilistic tractography (Behrens *et al.*, 2003b). Diffusion-weighted imaging (DWI) is able to characterize the apparent diffusion properties of water in different directions (Basser *et al.*, 1994). In an anisotropically organized structure such as the brain, local water diffusion is fastest along the predominant orientation of fibre tracts. DWI can therefore be used to infer these fibre orientations in white (Henkelman *et al.*, 1994; Conturo *et al.*, 1999; Jones *et al.*, 1999b; Mori *et al.*, 1999) or grey matter (Wiegell *et al.*, 2003). By classifying thalamic voxels according to the cortical region with which they show the highest connection probability, we can parcellate the thalamus into distinct 'connectivity-defined regions' (CDRs) that we hypothesize correspond to thalamic nuclei or nuclear groups (Behrens *et al.*, 2003a).

Here, we test the anatomical and functional validity of this correspondence more directly and begin to characterize the variability of CDRs across a healthy population. First, we produce group probability maps that express the population likelihood of connection to each cortical region for every point in the thalamus. Second, to test the correspondence between our CDRs and thalamic nuclei, we compare the relative volumes of our CDRs to cytoarchitectonically defined nuclear volumes from a previous histological atlas of the thalamus. Finally, we test the correspondence between our structurally defined thalamic parcellation and the localization of previously reported functional activations during motor or executive tasks. This not only serves to validate our approach, but also illustrates how information from the group probability atlas can be used to guide structure–function correlations.

Materials and Methods

Data Acquisition

Diffusion-weighted (DW) data were acquired in 11 healthy subjects (7 male, 4 female, mean age 34.9 ± 11.2 years) using echo planar imaging with optimized cardiac gating (Wheeler-Kingshott *et al.*, 2002) (60 × 2.3 mm thick slices, field of view = 220 × 220 mm^2, matrix = 96 × 96; reconstructed on 128 × 128 matrix giving final resolution of 1.7 × 1.7 × 2.3 mm^3) implemented on a General Electric 1.5 T Signa Horizon scanner with standard quadrature head-coil and maximum gradient strength of 22 mT/m. Informed written consent was obtained from all subjects in accordance with approval from the National Hospital for Neurology and Neurosurgery and the Institute of Neurology Joint Research Ethics Committee. The diffusion weighting was isotropically distributed along 54 directions (δ = 34 ms, Δ = 40 ms, *b*-value = 1150 s/mm; Jones *et al.*, 1999a). Six diffusion-weighted volumes (*b*-value = 300 s/mm) and six volumes with no diffusion weighting were acquired.

In each subject, a high-resolution T_1-weighted scan was obtained with a 3-D inversion recovery prepared spoiled gradient echo (IR-SPGR;

FOV = 310 × 155; matrix = 256 × 128; in-plane resolution = 1.2 × 1.2 mm^2; 156 × 1.2 mm thick slices; T_I = 450 ms; T_R = 2 s; T_E = 53 ms).

Image Analysis

Probabilistic diffusion tractography was carried out according to previously detailed methods (Behrens *et al.*, 2003a,b). Using Bayesian techniques, we estimate a probability distribution function (pdf) on the principal fibre direction at each voxel. We then generate probability distributions of connectivity between seed and all other points by repeatedly sampling connected pathways through this pdf field. The effect of this procedure is to build a probability distribution on the location of the dominant connection from the seed voxel.

We manually outlined the whole thalamus (creating a 'mask') and seven exclusive cortical regions [prefrontal (PFC), primary motor (M1), premotor (lateral and medial) (PMC), temporal, posterior parietal (PPC), primary and secondary somatosensory (S1/S2) and occipital cortices; Fig. 1*Aiii*] on each subject's T_1-weighted image using anatomical landmarks detailed previously (Behrens *et al.*, 2003a). For tissue-type segmentation, skull stripping and registration, tools from the FMRIB Software Library (FSL; www.fmrib.ox.ac.uk/fsl) were used. We performed probabilistic tissue type segmentation and partial volume estimation on the T_1-weighted image (Zhang *et al.*, 2001) and masked cortical regions to include only voxels estimated at >15% grey matter. We skull-stripped (Smith, 2002) diffusion-weighted, T_1-weighted and MNI standard brain template images (Evans *et al.*, 2003) and performed affine registration (Jenkinson and Smith, 2001) to derive transformation matrices between the three spaces.

From each voxel in the thalamus mask, we drew samples from the connectivity distribution and recorded the number of samples that passed through each cortical mask. For each thalamic voxel in standard space we calculated a probability of connection to each cortical zone as a proportion of the total number of samples from that voxel that reached any cortical area. Hard segmentation of the thalamus was performed by classifying seed voxels as connecting to the cortical mask with the highest connection probability, resulting in exclusive connectivity-defined regions (CDRs). For each cortical area, we thresholded and binarized individual subject results to include only those thalamic voxels with a connection probability >25%. These images were overlaid to create group probability maps of thalamic sub-regions.

In order to derive relative volumes of cytoarchitectonically defined nuclei we manually measured the cross-sectional area of major nuclei delineated in axial cytoarchitectonic slices from a single human brain (Schaltenbrand and Wahren, 1977) and multiplied by slice thickness to calculate the volume of each thalamic nucleus. Many of our cortical target regions are connected to more than one thalamic nucleus and many nuclei connect to more than one cortical target. Therefore, in order to estimate cytoarchitectonic-based volumes for the total region of the thalamus projecting to each of the seven cortical target regions, we combined the nuclear volumes into groups as follows: M1 (ventrolateral plus centremedian nuclei), PFC (anterior, mediodorsal and ventral anterior nuclei), PMC (ventral anterior nucleus), PPC (lateral posterior plus pulvinar nuclei), S1/S2 (ventral posterior lateral nucleus), temporal (pulvinar nucleus). Half of the volume of the ventral anterior nucleus was assigned to PFC and half to PMC. Similarly, the volume of the pulvinar was equally split between PPC and temporal targets. The volume of the individual subject DWI-based CDRs for each cortical target was found directly from our imaging data and averaged across subjects giving a single mean volume for each CDR. As we were interested in relative rather than absolute volumes, both cytoarchitectonic- and DWI-based measures were normalized to their respective maximum volumes. To test directly the correspondence between the

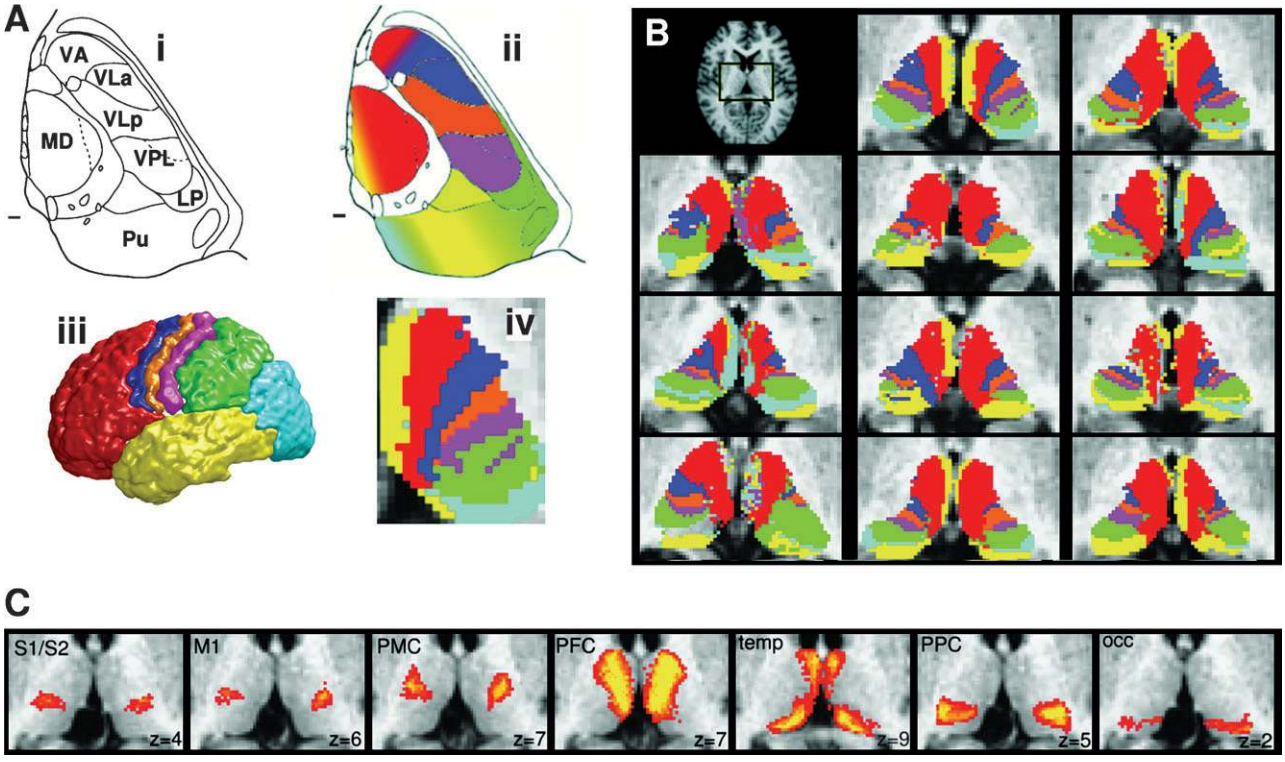

Figure 1. Individual variation of connectivity-based thalamic segmentation. (*A*) Segmentation of the human thalamus. (*i*) Axial thalamic section from a cytoarchitectonic atlas (Morel *et al.*, 1997). (*ii*) In the same atlas section, major nuclei have been coloured according to their major cortical connection site (as in iii). (*iii*) Cortical subdivisions. Red = PFC; blue = PMC; orange = M1; magenta = S1/S2; green = PPC; cyan = occipital; yellow = temporal. (*iv*) Connectivity-based parcellation of the thalamus in a single subject for an axial slice at the same level as the section in *A* and *B*. Voxels are coloured according to the cortical region with which they show the highest connection probability (as in *iii*). (*B*) Connectivity-based segmentation of the thalamus in eleven subjects. Top left panel indicates location of axial thalamic slices. Each subsequent panel represents data from an individual subject. Thalamic voxels colour coded as in *Aiii*. (*C*) Group probability maps. Axial images showing overlap of thalamic sub-regions across subjects in voxels showing >25% probability of connection to selected cortical mask (indicated in top left of each image) using a colour scale running from red (4/11 subjects) to yellow (11/11 subjects). Slices are taken at the average *Z*-coordinate (given in bottom right of each image) across the left and right hemispheres for the centre of gravity of that cluster.

seven volumes (one for each cortical target area) derived from the cytoarchitectonic atlas and the seven defined from DWI, we calculated the correlation between them using Pearson's correlation co-efficient with a one-tailed probability threshold of $P < 0.05$.

We compared the locations of group probability maps to centres of thalamic activations from functional imaging studies of upper limb movements and of executive tasks that activated the motor/premotor and prefrontal cortices, respectively. Studies for inclusion were identified by searching the PubMed database (http://www.ncbi.nlm.nih.gov/entrez/). We included BOLD fMRI or rCBF PET studies published between 1 January 1999 and 30 December 2003 in which coordinates of whole brain activation were reported for a group of at least five healthy human control subjects. We included only studies published in the following journals: *Neuroimage*, *Journal of Neuroscience*, *Cerebral Cortex*, *Proceedings of the National Academy of Science USA*, *Brain Research*, *Cognitive Brain Research*, *Neuron*, *Neuropsychologia*, *Journal of Cognitive Neuroscience*, *Brain* and *Experimental Brain Research*. To identify motor tasks that activated motor or premotor cortex, we used the search term *(fmri OR pet) AND ((motor OR sensorimotor OR premotor) AND cortex) AND movement AND (hand OR finger)*. Papers that reported activation for unilateral hand or finger motor tasks versus rest or a non-motor baseline, or activations that varied with a simple movement parameter (rate or force) were included. This identified a total of 38 studies that fulfilled our selection criteria. Of these, 24 did not report any thalamic activation for the contrasts of interest and 14 did report thalamic activations (of which two fell outside the thalamus). Twelve movement-related thalamic activations were therefore included in further analyses.

To identify executive/memory tasks that activated the prefrontal cortex we used the search term *(fmri OR pet) AND prefrontal AND ((planning) OR (n back) OR (wisconsin card sorting) OR (prospective memory) OR (source memory) OR ((task OR set) AND (switch OR switching OR shift)) OR (delayed response))*. Papers that reported activation for the cognitive tasks listed in this search time versus a control or rest baseline were included. This identified 59 studies that fulfilled our inclusion criteria. Of these, 41 did not report thalamic activation and 18 did report thalamic activation. The 18 studies with thalamic activation reported a total of 31 thalamic activation centres of which four fell outside the thalamus leaving 27 thalamic activation centres to enter into further analyses.

Coordinates from functional imaging studies are reported in MNI space (Evans *et al.*, 2003) and in cases where the MNI template was not originally used coordinates were converted using a simple non-linear transform (http://www.mrc-cbu.cam.ac.uk/Imaging/mnispace.html).

Results

Connectivity-based Anatomy: Probabilistic Segmentation

Classification of thalamic voxels based on the cortical region with which they showed the highest connection probability resulted in the definition of clusters of commonly-connected voxels whose relative locations correspond well to major thalamic nuclei (Fig. 1*A*). Qualitatively, the relative locations and extents of these individual connectivity-defined sub-regions (CDR) were reproducible across subjects (Fig. 1*B*). Although the relative positions of CDRs were preserved across subjects, there was some variability in the precise volumes and locations of borders (Fig. 1*B*). However, in these 'hard' segmentations, in which voxels are classified according to their highest cortical connection probability, the edges of clusters may depend on voxels that show only low probability of connection to any cortical region (e.g. from areas that have predominantly subcortical connections).

To characterize voxel-wise correspondence in thalamic connections across subjects quantitatively, we co-registered binarized masks of thalamic regions showing >25% probability of connection to each of the defined cortical areas. The resulting group probability maps are centred on localized regions of high probability (across the group) of connection to each cortical region (Fig. 1*C*). These results have been entered into a probabilistic atlas which is available at http://www.fmrib.ox.ac.uk/connect. Because the borders of these probability maps are intrinsically fuzzy, we used thresholded group maps to conveniently display boundaries between the sub-regions of the thalamus in a standard brain space (Fig. 2).

Volumetric Measurements

Having established evidence for between-subject reproducibility of our thalamic parcellation, we further tested the hypothesis that the sub-regions found in this way (i.e. the individual subject CDRs) correspond to thalamic nuclei or nuclear groups. The correspondence between the relative locations of our CDRs and cytoarchitectonically defined nuclei in the thalamus post-mortem (Fig. 1*A*) supports this claim. We also compared the mean relative volumes of individual CDRs and cytoarchitectonically defined nuclear groups. We found a strong correlation between the mean relative volume across subjects defined using DWI and those based on a cytoarchitectonic atlas (Fig. 3*A*, left hemisphere $r = 0.71$, $P = 0.038$; right hemisphere $r = 0.70$, $P = 0.04$).

Overlapping Connections to Multiple Cortical Areas

The analysis thus far has considered only the primary cortical connection of each CDR. However, many of the voxels within CDRs generated connections to cortical regions other than their primary cortical target. Quantitative expression of connection probability allows us also to characterize anatomically overlapping connectivities. The connectivity profiles of CDRs are highly reproducible across hemispheres and demonstrate that when CDRs show connectivity to multiple cortical regions these regions tend to be functionally related and/or physically adjacent (see online Supplementary Material). For example, the CDR with primary motor connections also has strong connections to premotor and somatosensory cortices. The existence of multiple cortical connections from each CDR could reflect multiple factors. A likely contributing factor is the fuzzy borders between cortical regions. However, an additional factor might be genuine interdigitation of regions within the thalamus connecting to disparate cortical areas. This could, for example, reflect the different distributions within the thalamus of distinct cell types with diffuse and specific cortical connections — so-called matrix and core neurons (Jones, 2001). We found evidence for interdigitation in the distribution of thalamic connections to PFC. Examination of the group mean probability map for connections to M1 and PFC from the thalamus demonstrates that the region connecting to PFC does not simply blur into the region connecting to M1. Rather, there are two distinct areas with PFC connections — a primary one that probably includes the mediodorsal nucleus and a secondary region, located within a sub-region anatomically corresponding to the ventrolateral nucleus (Fig. 3*B*). To assess the reliability of this pattern of PFC connection apparent in the mean connection probability profile, we inspected the corresponding slice in all individual subjects and found that a pattern of dense medial PFC connection, followed by a region without PFC connection, followed by a second, more lateral/inferior region of PFC connection was present in six out of eleven subjects.

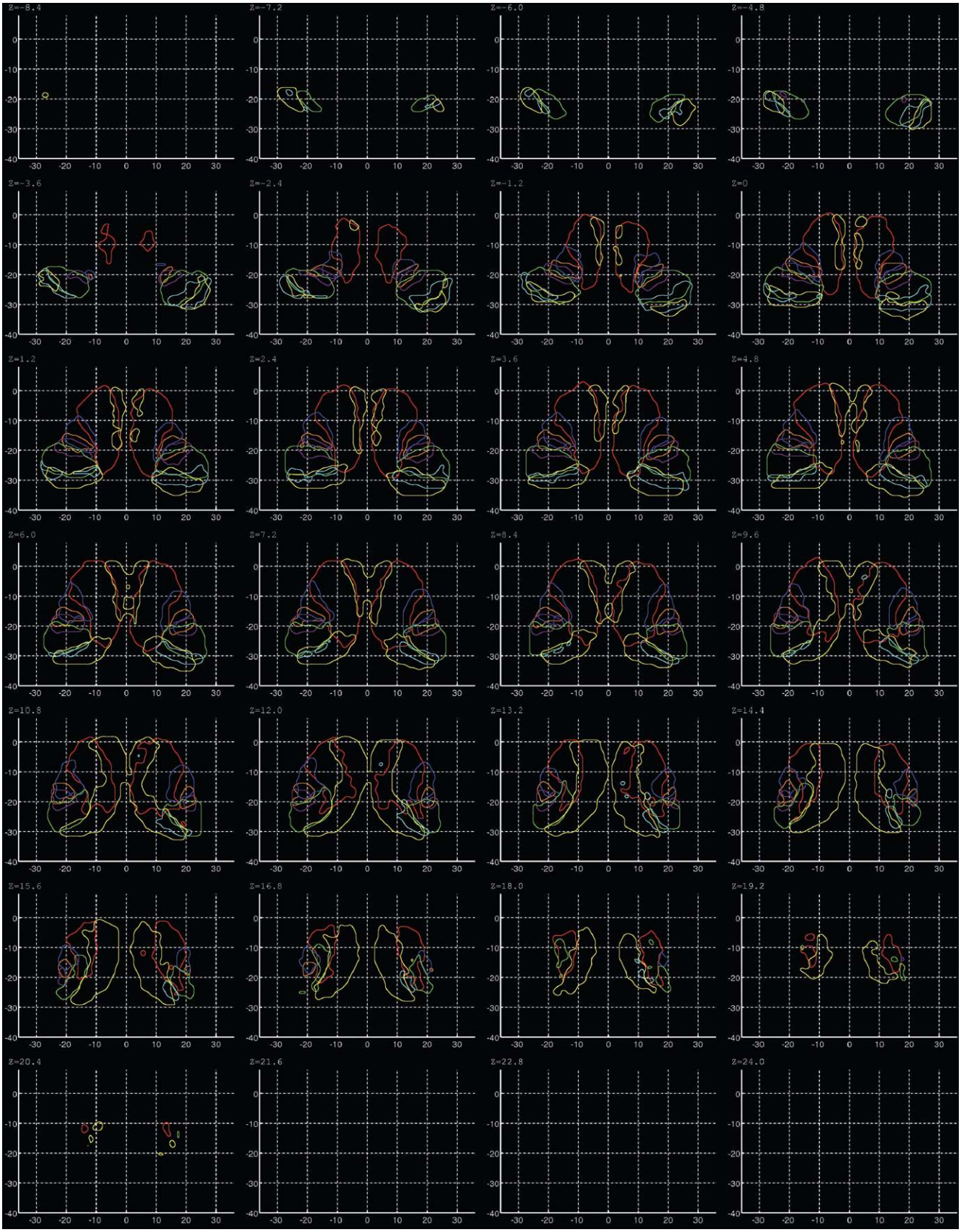

Figure 2. Thalamic connectivity atlas. Axial slices through the whole thalamus showing edges of thresholded (at >4/11 subjects) group probability maps for connection to each cortical region. Edges are coloured using the same scheme as in Figure 1*A*. *X*- and *Y*-axes give coordinates in standard (MNI) brain space. *Z*-coordinate of each slice is indicated in the top left corner. An interactive, probabilistic version of this atlas is available at http://www.fmrib.ox.ac.uk/connect

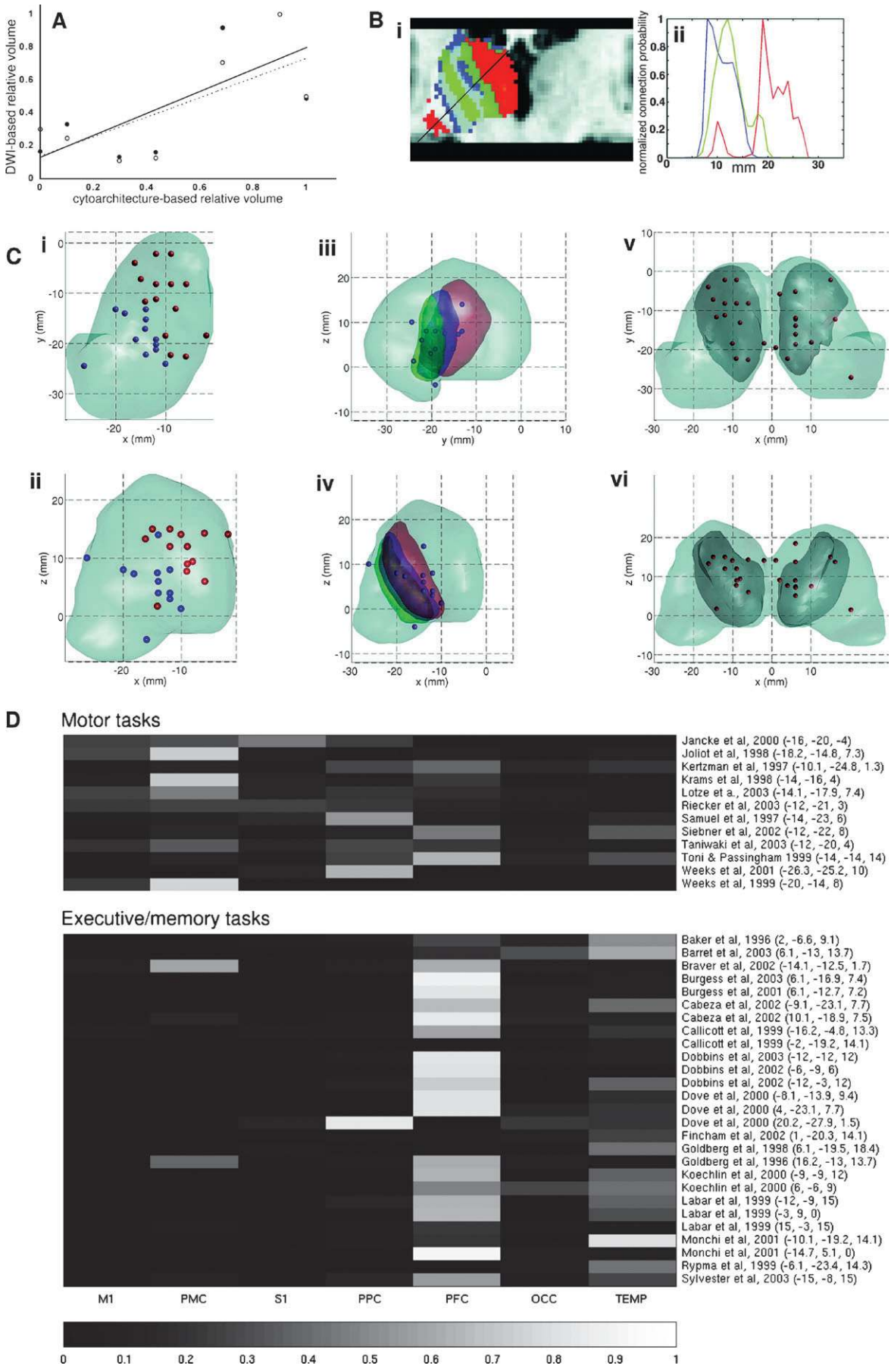

Co-localization with Centres of Functional Activation

We have proposed that the atlas based on our group probability maps could be used to assign likely anatomical labels to sites of brain activation or lesions. To test directly the functional–anatomical validity of the boundaries defined by our group maps, we assessed the correspondence between connectivity-defined volumes and previously reported centres of gravity of functional activations localized to the thalamus. Functional activations reported during motor and executive/memory tasks tended to cluster in distinct regions of the thalamus (Fig. 3*Ci,ii*). We used the atlas based on our group probability maps to characterize the connection probability profile for each functional activation centre (Fig. 3-D). Activation centres for the motor tasks tended to fall within regions of high probability of connection to sensorimotor and premotor areas (Fig. 3*Ciii,iv,D*). Similarly, activation centres for the executive and memory tasks fell within thalamic regions of high probability of connection to prefrontal cortex (Fig. 3*Cv,vi,D*).

Discussion

We provided evidence in support of the functional and anatomical validity of connectivity-based segmentations of the thalamus and characterized their variability. Previously we showed that diffusion tractography can be used to parcellate the thalamus into regions that we propose correspond to nuclei or nuclear groups (Behrens *et al.*, 2003a). Parcellations of the human thalamus based on cortical connectivity fit well with predictions based on invasive tract tracing studies on thalamocortical and cortico-thalamic connectivity in non-human animals (Jones, 1985; Goldman-Rakic and Porrino, 1985; Yeterian and Pandya, 1985, 1989, 1991, 1997; Darian-Smith *et al.*, 1990, 1996). Here we have defined the variation of human thalamic parcellation between individuals quantitatively by generating a probabilistic thalamic atlas. This was used to test more rigorously the hypothesis that the parcellation corresponds to functional anatomical divisions within the thalamus. First, we found good agreement between volumes of the thalamic sub-regions obtained using our method and comparable sub-regions from previous cytoarchitectonic data. Second, the locations of the individual regions correspond well with data from prior functional imaging experiments. We showed, for example, that thalamic activations with motor paradigms map into a region corresponding to the ventral lateral nucleus, while activations associated with tasks involving executive control and working memory co-localized with the connectivity-defined sub-region including the mediodorsal nucleus.

Parcellation of brain regions with respect to connectivity offers a complementary tool to conventional imaging of anatomical boundaries using tissue contrast arising from, e.g. differences in myeloarchitecture (Magnotta *et al.*, 2000). A notable feature of the current thalamic parcellation is that borders between regions are not sharp. In individual subject parcellations this may be due in part to genuinely fuzzy borders between thalamic regions or their cortical targets (e.g. connectivity to primary and premotor cortices from the ventral lateral and ventral lateral anterior nuclei). In addition, for many of the major relay nuclei of the thalamus, inputs are predominantly subcortical rather than cortical and even for nuclei with strong cortical connectivities, the distribution of these connectivities is based on cortical units (e.g. cytoarchitectonic regions, cortical layers) smaller than the large cortical regions used here (Goldman-Rakic and Porrino, 1985; Jones, 2001). Therefore, nuclear boundaries cannot always be expected to precisely match boundaries defined solely on the basis of cortical connectivity at the level used here.

Methodological factors, such as the limited spatial resolution and motion artefacts caused by pulsation of the cerebrospinal fluid in the third ventricle, will also contribute to the fuzziness of borders in our parcellation. Note, however, that as the tractography algorithm considers diffusion measurements not only within a voxel but also at a more global scale (Behrens *et al.*, 2003b), the effective resolution of our parcellation will be finer than that of the original diffusion images. The lack of sharp borders in the group probability maps will additionally reflect inter-individual variability in thalamic anatomy. Previous cytoarchitectonic studies have demonstrated variability in nuclear size and location between individuals (Morel *et al.*, 1997). Inter-individual variation in connectivity-defined parcellations will also reflect difficulties in precisely matching variations in brain and thalamic sizes and shapes in registration of images across the group. Finally, even within an individual, distortions and low spatial resolution in the EPI images limit the degree to which the high resolution structural and diffusion tractography images can be matched spatially. Here, we used a linear registration algorithm (Jenkinson and Smith, 2001). It could be argued that linear registration is preferable if the aim is to characterize anatomical variability. However, an alternative approach would be to use non-linear methods to match the external borders of the thalamus across subjects and then focus on variability in connectivity-defined intrinsic boundaries.

It has previously been difficult to validate directly diffusion tractography due to a lack of alternative methods providing

Figure 3. Functional–anatomical validation. (*A*) Correspondence between relative volumes based on cytoarchitectonic data and on DWI. Data are shown for the left (filled circles) and right (open circles) hemispheres. Regression lines are shown for the left (solid line) and right (dashed line) hemisphere data separately. DWI-based values are for individual CDR volumes averaged across subjects and normalized to the maximum average volume. (*B*) Overlap between prefrontal and motor cortical connections. (i) Coronal slice showing group mean probability of connection to M1 (blue to turquoise) and prefrontal cortex (red to yellow). Areas with overlapping connections to both cortical targets are shown in green. The region connecting to PFC does not simply blur into the region connecting to M1. (ii) 2D intensity profile along line indicated in *A*. Connection probabilities for M1 (blue line), PFC (red line) and PMC (green line) have been normalized by dividing by the maximum connection probability along the intensity trajectory for each cortical target. This profile emphasizes the existence of two distinct thalamic sub-regions projecting to prefrontal cortex. (*C*) Correspondence between connectivity-defined and functionally defined thalamic sub-regions. In each figure the light grey surface represents the whole thalamus, within which spheres represent centres of functional activations (see *D*) and volumes showing where at least 4/11 subjects had >25% probability of connection to particular cortical targets are represented as semi-transparent surfaces. (*i, ii*) Activation centres for motor tasks (blue) and executive/memory tasks (red) tended to be located in distinct regions of the thalamus. (*iii, iv*) Centres of thalamic activation for movement tasks and volumes with high probability of connection to primary motor cortex (blue), somatosensory cortex (green) and premotor cortex (red). [note that the coordinate from Taniwaki *et al.* (2003), which used left hand movements, has been reflected about the midline]. (*v, vi*) Centres of activation for executive and memory tasks and the volume with high probability of connection to prefrontal cortex (dark grey). Note that some studies provided more than one activation location (see *D*). (*D*) Connectivity probability profiles for functional activation centres. Each row in the figure represents one activation centre. Columns in the figure represent the seven cortical targets. The brightness of each cell represents the probability of connection to that cortical target ranging from zero (black) to one (white). Movement-related activations tend to have high probabilities of connection to sensorimotor, premotor and parietal cortices. Executive and memory tasks tend to have very specific high probability of connection to prefrontal cortex. It is clear that the motor and executive/memory activations have very different connection profiles.

similar data in humans, as well as the relative paucity of animal imaging data. Here we took two approaches to validation of the connectivity-based parcellation: first by comparison to cytoarchitectonic atlases and second by comparison to functional activations.

The demonstration that relative locations and volumes defined using a connectivity-based parcellation of the thalamus generally correspond well with volumetric measurements from cytoarchitectonic maps is a powerful test of the ability of the method to define correct targets and, by implication, to identify appropriate paths. We would not expect the absolute volumes to correspond between these two methods. While cytoarchitectonic measurements were made up only of volumes from major nuclei, the measurements based on diffusion imaging would have included contributions from smaller nuclei and from white matter regions within the thalamic volume. Therefore, not unexpectedly, the absolute volumes of sub-regions are greater for the connectivity based measures. Differences in relative volumes may also reflect technical factors that will result in varying sensitivity to different anatomical pathways. The diffusion tractography approach used here is sensitive primarily to major pathways and therefore smaller pathways, pathways with sharp path inflections or pathways that cross other tracts are not always detected. This may explain the relatively small size of the motor nucleus by our method compared to cytoarchitectonic measurements: pathways reaching the lateral parts of the motor strip from the thalamus would have to cross the superior longitudinal fasiculus and therefore may not be detected. Future work should assess quantitatively the correspondence between the locations of connectivity-defined CDRs and thalamic nuclei by comparison of centres and extents of such regions in standard stereotactic space. Such comparisons, however, are not straightforward, as there is unlikely to be a one-to-one correspondence between individual nuclei and CDRs (e.g. the CDR connecting to the posterior parietal cortex is likely to include regions of both the lateral posterior nuclei and parts of the pulvinar.)

Relating the thalamic parcellation to locations of centres of functional activations offers an alternative approach to its validation (and also illustrates an important potential application of the parcellation method). Although thalamic activation is frequently reported in imaging studies (Baker *et al.*, 1996; Davis *et al.*, 1998; LaBar *et al.*, 1999; Dove *et al.*, 2000; McGonigle *et al.*, 2000; Gerardin *et al.*, 2003), authors rarely assign activations to a specific nucleus, due to the problems of inferring nucleic architecture with current approaches. Here we have chosen to test the functional validity of connectivity-defined volumes with data from well-characterized tasks to minimize confounds in interpretation. Centres of activation associated with two distinct types of tasks showed good functional–anatomical correspondences: motor activations co-localized to the sub-region corresponding to the ventrolateral nucleus and activations during executive tasks were mainly located within the sub-region corresponding to the mediodorsal nucleus. The atlas based on our group maps presented here can be used to assign a probabilistic anatomical label to activation foci within the thalamus more generally. This could prove particularly useful in cases where functional connectivity between the thalamus and neocortex is otherwise ambiguous. For example, although thalamic activation is frequently reported in studies of pain (Davis *et al.*, 1998; Becerra *et al.*, 1999; DaSilva *et al.*, 2002), the nature of the thalamic processing remains unclear and would be illuminated substantially by a clarification of precisely which thalamic nuclei are involved in processing nociceptive versus non-nociceptive stimulation in the human brain.

The ability to perform probabilistic grey matter parcellation *in vivo* also raises new possibilities for the study of the brain in disease. The fact that connectivity-based segmentation of the thalamus is reproducible across a group of healthy individuals demonstrates the feasibility of this approach for study of disorders with putative thalamic pathology. Connectivity between the thalamus and prefrontal cortex is hypothesized to play a role in schizophrenia, for example (Andreasen *et al.*, 1996). The relative size and location of the thalamic sub-region with a high probability of connection to prefrontal cortex could be directly compared between schizophrenic subjects and healthy controls. Lesions of the thalamus itself can cause a variety of cognitive impairments and it has been suggested that particular impairments relate to specific nuclear damage, e.g. lesions to the mediodorsal nucleus are associated with executive dysfunction whereas lesions involving the intralaminar nuclei lead to impairments in attention (Van der Werf *et al.*, 2003). Localizing lesion sites on the group probability maps presented here would enable the generation of hypotheses concerning the likely thalamo-cortical pathways affected and enable more precise clinico-anatomical correlations to be made.

Supplementary Material

Supplementary material can be found at:
http://www.cercor.oupjournals.org/

Notes

We acknowledge the support of the Wellcome Trust (H.J.B.), UK Medical Research Council (P.M.M.), UK Engineering and Physical Science Research Council (T.E.J.B., S.M.S.) and Multiple Sclerosis Society of Great Britain and Northern Ireland (P.M.M.). We are grateful to D. Mortimer and D. Flitney for assistance with figures and the web-based atlas, K. Sheehan for masking, C. Wheeler-Kingshott, G. Barker and P. Boulby for data acquisition, J.M. Brady for invaluable supervision (T.E.B.) and an anonymous reviewer for useful suggestions for improving the manuscript.

Address correspondence to Dr Heidi Johansen-Berg, Centre for Functional Magnetic Resonance Imaging of the Brain, John Radcliffe Hospital, Headley Way, Oxford OX3 9DU, UK. Email: heidi@fmrib.ox.ac.uk.

References

Andreasen NC, O'Leary DS, Cizadlo T, Arndt S, Rezai K, Ponto LL, Watkins GL, Hichwa RD (1996) Schizophrenia and cognitive dysmetria: a positron-emission tomography study of dysfunctional prefrontal-thalamic-cerebellar circuitry. Proc Natl Acad Sci USA 93: 9985–9990.

Baker SC, Rogers RD, Owen AM, Frith CD, Dolan RJ, Frackowiak RS, Robbins TW (1996) Neural systems engaged by planning: a PET study of the Tower of London task. Neuropsychologia 34:515–526.

Barrett NA, Large MM, Smith GL, Karayanidis F, Michie PT, Kavanagh DJ, Fawdry R, Henderson D, O'Sullivan BT (2003) Human brain regions required for the dividing and switching of attention between two features of a single object. Brain Res Cogn Brain Res 17:1–13.

Basser PJ, Mattiello J, LeBihan D (1994) MR diffusion tensor spectroscopy and imaging. Biophys J 66:259–267.

Becerra LR, Breiter HC, Stojanovic M, Fishman S, Edwards A, Comite AR, Gonzalez RG, Borsook D (1999) Human brain activation under controlled thermal stimulation and habituation to noxious heat: an fMRI study. Magn Reson Med 41:1044–1057.

Behrens TEJ, Johansen-Berg H, Woolrich MW, Smith SM, Wheeler-Kingshott CA, Boulby PA, Barker GJ, Sillery EL, Sheehan K, Ciccarelli O, Thompson AJ, Brady JM, Matthews PM (2003a) Non-invasive

mapping of connections between human thalamus and cortex using diffusion imaging. Nat Neurosci 6:750–757.
Behrens TEJ, Woolrich MW, Jenkinson M, Johansen-Berg H, Nunes RG, Clare S, Matthews PM, Brady JM, Smith SM (2003b) Characterization and propagation of uncertainty in diffusion-weighted MR imaging. Magn Reson Med 50:1077–1088.
Braver TS, Bongiolatti SR (2002) The role of frontopolar cortex in subgoal processing during working memory. Neuroimage 15: 523–536.
Burgess PW, Quayle A, Frith CD (2001) Brain regions involved in prospective memory as determined by positron emission tomography. Neuropsychologia 39:545–555.
Burgess PW, Scott SK, Frith CD (2003) The role of the rostral frontal cortex (area 10) in prospective memory: a lateral versus medial dissociation. Neuropsychologia 41:906–918.
Cabeza R, Dolcos F, Graham R, Nyberg L (2002) Similarities and differences in the neural correlates of episodic memory retrieval and working memory. Neuroimage 16:317–330.
Callicott JH, Mattay VS, Bertolino A, Finn K, Coppola R, Frank JA, Goldberg TE, Weinberger DR (1999) Physiological characteristics of capacity constraints in working memory as revealed by functional MRI. Cereb Cortex 9:20–26.
Conturo TE, Lori NF, Cull TS, Akbudak E, Snyder AZ, Shimony JS, McKinstry RC, Burton H, Raichle ME (1999) Tracking neuronal fiber pathways in the living human brain. Proc Natl Acad Sci USA 96:10422–10427.
Darian-Smith C, Darian-Smith I, Cheema SS (1990) Thalamic projections to sensorimotor cortex in the macaque monkey: use of multiple retrograde fluorescent tracers. J Comp Neurol 299:17–46.
Darian-Smith I, Galea MP, Darian-Smith C, Sugitani M, Tan A, Burman K (1996) The anatomy of manual dexterity. The new connectivity of the primate sensorimotor thalamus and cerebral cortex. Adv Anat Embryol Cell Biol 133:1–140.
DaSilva AF, Becerra L, Makris N, Strassman AM, Gonzalez RG, Geatrakis N, Borsook D (2002) Somatotopic activation in the human trigeminal pain pathway. J Neurosci 22:8183–8192.
Davis KD, Kwan CL, Crawley AP, Mikulis DJ (1998) Functional MRI study of thalamic and cortical activations evoked by cutaneous heat, cold, tactile stimuli. J Neurophysiol 80:1533–1546.
Dobbins IG, Foley H, Schacter DL, Wagner AD (2002) Executive control during episodic retrieval: multiple prefrontal processes subserve source memory. Neuron 35:989–996.
Dobbins IG, Rice HJ, Wagner AD, Schacter DL (2003) Memory orientation and success: separable neurocognitive components underlying episodic recognition. Neuropsychologia 41:318–333.
Dove A, Pollmann S, Schubert T, Wiggins CJ, von Cramon DY (2000) Prefrontal cortex activation in task switching: an event-related fMRI study. Brain Res Cogn Brain Res 9:103–109.
Evans AC, Collins DL, Mills SR, Brown ED, Kelly RL, Peters TM (2003) 3-D statistical neuroanatomical models from 305 MRI volumes. Proc IEEE Symp 95:1813–1817.
Fincham JM, Carter CS, van Veen V, Stenger VA, Anderson JR (2002) Neural mechanisms of planning: a computational analysis using event-related fMRI. Proc Natl Acad Sci USA 99:3346–3351.
Gerardin E, Lehericy S, Pochon JB, Tezenas du MS, Mangin JF, Poupon F, Agid Y, Le Bihan D, Marsault C (2003) Foot, hand, face and eye representation in the human striatum. Cereb Cortex 13:162–169.
Goldberg TE, Berman KF, Randolph C, Gold JM, Weinberger DR (1996) Isolating the mnemonic component in spatial delayed response: a controlled PET ^{15}O-labeled water regional cerebral blood flow study in normal humans. Neuroimage 3:69–78.
Goldberg TE, Berman KF, Fleming K, Ostrem J, Van Horn JD, Esposito G, Mattay VS, Gold JM, Weinberger DR (1998) Uncoupling cognitive workload and prefrontal cortical physiology: a PET rCBF study. Neuroimage 7:296–303.
Goldman-Rakic PS, Porrino LJ (1985) The primate mediodorsal (MD) nucleus and its projection to the frontal lobe. J Comp Neurol 242:535–560.
Guillery RW, Sherman SM (2002) Thalamic relay functions and their role in corticocortical communication: generalizations from the visual system. Neuron 33:163–175.
Henkelman RM, Stanisz GJ, Kim JK, Bronskill MJ (1994) Anisotropy of NMR properties of tissues. Magn Reson Med 32:592–601.
Jancke L, Loose R, Lutz K, Specht K, Shah NJ (2000) Cortical activations during paced finger-tapping applying visual and auditory pacing stimuli. Brain Res Cogn Brain Res 10:51–66.
Jenkinson M, Smith S (2001) Global optimisation for robust affine registration. Med Image Anal 5:143–156.
Joliot M, Crivello F, Badier JM, Diallo B, Tzourio N, Mazoyer B (1998) Anatomical congruence of metabolic and electromagnetic activation signals during a self-paced motor task: a combined PET-MEG study. Neuroimage 7:337–351.
Jones DK, Horsfield MA, Simmons A (1999a) Optimal strategies for measuring diffusion in anisotropic systems by magnetic resonance imaging. Magn Reson Med 42:515–525.
Jones DK, Simmons A, Williams SC, Horsfield MA (1999b) Non-invasive assessment of axonal fiber connectivity in the human brain via diffusion tensor MRI. Magn Reson Med 42:37–41.
Jones EG (1985) The thalamus. New York: Plenum Press.
Jones EG (2001) The thalamic matrix and thalamocortical synchrony. Trends Neurosci 24:595–601.
Kertzman C, Schwarz U, Zeffiro TA, Hallett M (1997) The role of posterior parietal cortex in visually guided reaching movements in humans. Exp Brain Res 114:170–183.
Koechlin E, Corrado G, Pietrini P, Grafman J (2000) Dissociating the role of the medial and lateral anterior prefrontal cortex in human planning. Proc Natl Acad Sci USA 97:7651–7656.
Krams M, Rushworth MF, Deiber MP, Frackowiak RS, Passingham RE (1998) The preparation, execution and suppression of copied movements in the human brain. Exp Brain Res 120:386–398.
LaBar KS, Gitelman DR, Parrish TB, Mesulam M (1999) Neuroanatomic overlap of working memory and spatial attention networks: a functional MRI comparison within subjects. Neuroimage 10:695–704.
Lotze M, Braun C, Birbaumer N, Anders S, Cohen LG (2003) Motor learning elicited by voluntary drive. Brain 126:866–872.
McGonigle DJ, Howseman AM, Athwal BS, Friston KJ, Frackowiak RS, Holmes AP (2000) Variability in fMRI: an examination of intersession differences. Neuroimage 11:708–734.
Magnotta VA, Gold S, Andreasen NC, Ehrhardt JC, Yuh WT (2000) Visualization of subthalamic nuclei with cortex attenuated inversion recovery MR imaging. Neuroimage 11:341–346.
Modell JG, Mountz JM, Curtis GC, Greden JF (1989) Neurophysiologic dysfunction in basal ganglia/limbic striatal and thalamocortical circuits as a pathogenetic mechanism of obsessive-compulsive disorder. J Neuropsychiatry Clin Neurosci 1:27–36.
Monchi O, Petrides M, Petre V, Worsley K, Dagher A (2001) Wisconsin Card Sorting revisited: distinct neural circuits participating in different stages of the task identified by event-related functional magnetic resonance imaging. J Neurosci 21:7733–7741.
Morel A, Magnin M, Jeanmonod D (1997) Multiarchitectonic and stereotactic atlas of the human thalamus. J Comp Neurol 387: 588–630.
Mori S, Crain BJ, Chacko VP, van Zijl PC (1999) Three-dimensional tracking of axonal projections in the brain by magnetic resonance imaging. Ann Neurol 45:265–269.
Riecker A, Wildgruber D, Mathiak K, Grodd W, Ackermann H (2003) Parametric analysis of rate-dependent hemodynamic response functions of cortical and subcortical brain structures during auditorily cued finger tapping: a fMRI study. Neuroimage 18:731–739.
Rypma B, Prabhakaran V, Desmond JE, Glover GH, Gabrieli JD (1999) Load-dependent roles of frontal brain regions in the maintenance of working memory. Neuroimage 9:216–226.
Samuel M, Ceballos-Baumann AO, Blin J, Uema T, Boecker H, Passingham RE, Brooks DJ (1997) Evidence for lateral premotor and parietal overactivity in Parkinson's disease during sequential and bimanual movements. A PET study. Brain 120:963–976.
Schaltenbrand G and Wahren W (1977) Atlas for stereotaxy of the human brain. Stuttgart: Thieme.
Siebner HR, Limmer C, Peinemann A, Drzezga A, Bloem BR, Schwaiger M, Conrad B (2002) Long-term consequences of switching handedness: a positron emission tomography study on handwriting in 'converted' left-handers. J Neurosci 22:2816–2825.

Smith SM (2002) Fast robust automated brain extraction. Hum Brain Mapp 17:143–155.
Sylvester CY, Wager TD, Lacey SC, Hernandez L, Nichols TE, Smith EE, Jonides J (2003) Switching attention and resolving interference: fMRI measures of executive functions. Neuropsychologia 41: 357–370.
Taniwaki T, Okayama A, Yoshiura T, Nakamura Y, Goto Y, Kira J, Tobimatsu S (2003) Reappraisal of the motor role of basal ganglia: a functional magnetic resonance image study. J Neurosci 23: 3432–3438.
Toni I, Passingham RE (1999) Prefrontal–basal ganglia pathways are involved in the learning of arbitrary visuomotor associations: a PET study. Exp Brain Res 127:19–32.
Van Buren JM, Burke RC (1972) Variations and connections of the human thalamus. 1. The nuclei and cerebral connections of the human thalamus. New York: Springer-Verlag.
Van der Werf YD, Scheltens P, Lindeboom J, Witter MP, Uylings HB, Jolles J (2003) Deficits of memory, executive functioning and attention following infarction in the thalamus; a study of 22 cases with localised lesions. Neuropsychologia 41:1330–1344.
von Cramon DY, Hebel N, Schuri U (1985) A contribution to the anatomical basis of thalamic amnesia. Brain 108:993–1008.
Wallesch CW, Kornhuber HH, Kunz T, Brunner RJ (1983) Neuropsychological deficits associated with small unilateral thalamic lesions. Brain 106:141–152.
Weeks RA, Gerloff C, Dalakas M, Hallett M (1999) PET study of visually and non-visually guided finger movements in patients with severe pan-sensory neuropathies and healthy controls. Exp Brain Res 128:291–302.
Weeks RA, Honda M, Catalan MJ, Hallett M (2001) Comparison of auditory, somatosensory, visually instructed and internally generated finger movements: a PET study. Neuroimage 14:219–230.
Wheeler-Kingshott CA, Boulby PA, Symms M, Barker GJ (2002) Optimized cardiac gating for high-resolution whole brain DTI on a standard scanner. Proc Intl Soc Mag Reson Med 10:1118.
Wiegell MR, Tuch DS, Larsson HB, Wedeen VJ (2003) Automatic segmentation of thalamic nuclei from diffusion tensor magnetic resonance imaging. Neuroimage 19:391–401.
Yeterian EH, Pandya DN (1985) Corticothalamic connections of the posterior parietal cortex in the rhesus monkey. J Comp Neurol 237:408–426.
Yeterian EH, Pandya DN (1988) Corticothalamic connections of paralimbic regions in the rhesus monkey. J Comp Neurol 269:130–146.
Yeterian EH, Pandya DN (1989) Thalamic connections of the cortex of the superior temporal sulcus in the rhesus monkey. J Comp Neurol 282:80–97.
Yeterian EH, Pandya DN (1991) Corticothalamic connections of the superior temporal sulcus in rhesus monkeys. Exp Brain Res 83:268–284.
Yeterian EH, Pandya DN (1997) Corticothalamic connections of extrastriate visual areas in rhesus monkeys. J Comp Neurol 378: 562–585.
Zhang Y, Brady M, Smith S (2001) Segmentation of brain MR images through a hidden Markov random field model and the expectation-maximization algorithm. IEEE Trans Med Imaging 20:45–57.